Lawrence Berkeley Laboratory
UNIVERSITY OF CALIFORNIA

Accelerator & Fusion
Research Division

LBL--21348

DE87 000058

Presented at the 1986 International Symposium on
Heavy Ion Fusion, Washington, DC,
May 27-29, 1986

PRELIMINARY RESULTS FROM MBE-4: A FOUR BEAM INDUCTION LINAC FOR HEAVY ION FUSION RESEARCH

T.J. Fessenden, D.L. Judd, D. Keefe, C. Kim,
L.J. Laslett, L. Smith, and A.I. Warwick

May 1986

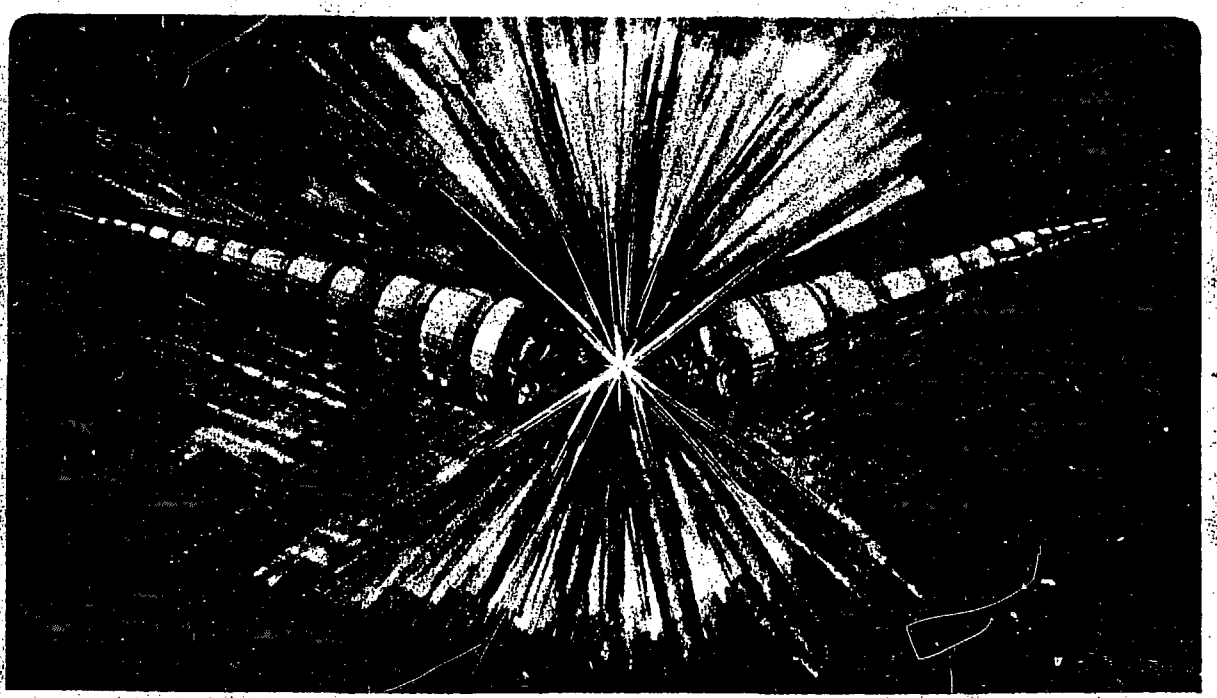

Prepared for the U.S. Department of Energy under Contract DE-AC03-76SF00098

LBL-21348
HIFAN-316

LBL--21348

DE87 000058

PRELIMINARY RESULTS FROM MBE-4: A FOUR BEAM INDUCTION LINAC FOR HEAVY ION FUSION RESEARCH*

T.J. Fessenden, D.L. Judd, D. Keefe, C. Kim, L.J. Laslett
L. Smith, and A.I. Warwick

Lawrence Berkeley Laboratory
University of California
Berkeley, California 94720

May 1986

DISCLAIMER

---

* This work was supported by the Office of Energy Research, Office of Basic Sciences, U.S. Department of Energy under Contract No. DE-AC03-76SF00098.

PRELIMINARY RESULTS FROM MBE-4: A FOUR BEAM INDUCTION LINAC FOR HEAVY ION FUSION RESEARCH*

T.J. Fessenden, D.L. Judd, D. Keefe, C. Kim, L.J. Laslett
L. Smith, and A.I. Warwick

Lawrence Berkeley Laboratory
University of California, Berkeley, CA 94720

Presented by A.I. Warwick

ABSTRACT

Preliminary results are presented from a scaled experimental multiple beam induction linac. This experiment is part of a program of accelerator research for heavy ion fusion. It is shown that multiple beams can be accelerated without significant mutual interaction. Measurements of the longitudinal dynamics of a current-amplifying induction linac are presented and compared to calculations. Coupling of transverse and longitudinal dynamics is discussed.

INTRODUCTION

MBE-4 is an experimental multiple beam ion induction linac which will model on a small scale some of the beam dynamics of a much larger fusion driver. About half the linac is constructed and operational at this time and we present preliminary analyses of the behaviour of the beams.

Four space-charge-dominated beams of Cs^+ ions, initially at 200 keV and with initial currents of 11 mA each, are individually focussed by electrostatic quadrupoles and accelerated, with current amplification, by fields induced when high voltage pulsers discharge through carefully designed circuits looping the induction cores. Figure 1 shows the layout of the linac; at present sections A and B are operational. Overall design details and the performance of the 4-beam injector have been presented at the 1985 Particle Accelerator Conference.[1] The beam envelopes are matched into the quadrupole lattice during transport through the conditioning section.[2] In this paper we will discuss acceleration through sections A and B.

An induction linac fusion driver is likely to have a large number of beams which will be accelerated and amplified in current by shaped induced fields. A number of issues arise, of which the following will be addressed by MBE-4:

a) MBE-4 can demonstrate the principle of a multiple beam linac.

b) Acceleration and current amplification by means of shaped voltage pulses can be demonstrated, requiring successful design and operation of the high voltage pulsers.

*This work was supported by the Office of Energy Research, Office of Basic Energy Sciences, U.S. Department of Energy under Contract No. DE-AC03-76SF00098.

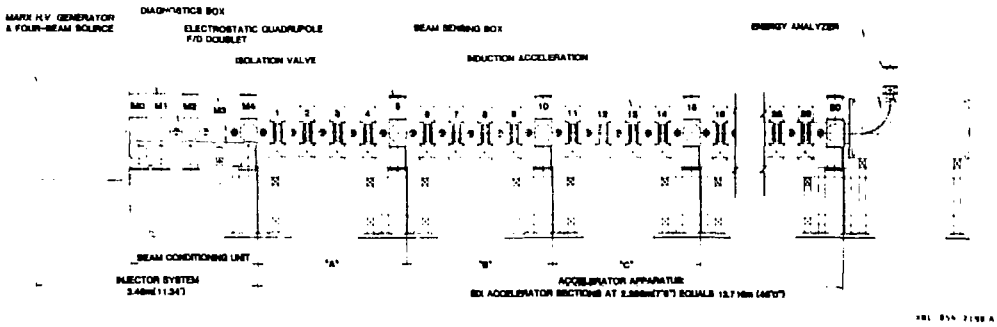

Fig. 1. Complete layout of the MBE-4 accelerator.

c) Because of the low ion velocity, current amplification schedules can be implemented which are more ambitious than any contemplated for a driver. In the 17 m length of MBE-4 it should be possible to model the longitudinal dynamics of a significantly longer portion of a large accelerator.

d) The ends of the bunch must be held together against the effects of longitudinal space charge forces.

e) The effect of longitudinal manipulations can be investigated. They should cause acceptably small growth of the longitudinal emittance.

f) Transverse emittance can be measured to see if it is conserved over the length of the experiment during acceleration.

g) Coupling of the transverse and longitudinal dynamics can be investigated in terms of the envelope oscillations induced during acceleration.

MULTIPLE BEAM EFFECTS

The four beams of MBE-4 are not expected to interact in any significant way during transport and acceleration. The only location where they deflect one another is at the emitter surface of the thermionic ion source. Here the ions are moving slowly and the charge density in the beams is high. The design computations indicated a deflection between beams of a few milliradians which was approximately compensated by shaping the anode and eliminated during initial operation by shimming.

Figure 2 shows current density profiles for a drifting beam at gap 5, both in the presence and absence of the other three beams. There is no appreciable difference. These profiles are measured by moving a small hole (.5 mm x .5 mm) across the center of the beam and sensing the transmitted current.

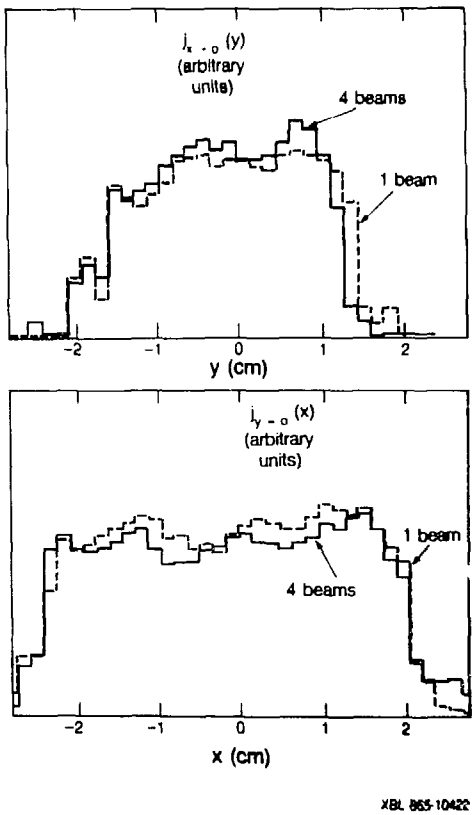

Fig. 2. Horizontal and vertical current density profiles of the bottom beam at the end of section A (gap 5). The profiles measured under normal operation (4 beams) are compared with those measured when the other three beams are blocked at gap 0 (1 beam)

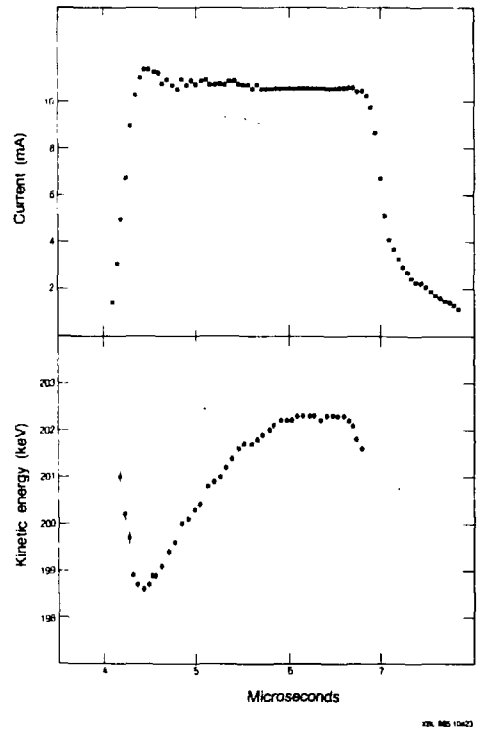

Fig. 3. Initial conditions for acceleration and current amplification; current and kinetic energy measured at the beginning of section A (gap 0)

LONGITUDINAL DYNAMICS

Figure 3 shows the measured initial current and kinetic energy waveforms of one of the beam bunches at the diagnostic location immediately before accelerator section A (gap 0). These data are the starting point for the design of the accelerating schedule. Of immediate concern is the non-uniform kinetic energy waveform produced by the Marx pulse on the diode. Ions take 500 ns to cross the diode gap at 200 kV. There is a transient during the first and last 500 ns of the pulse as the diode fills with, and empties of, charge. It is necessary to precisely shape the rising edge of the 200 kV Marx pulse to minimize current and kinetic energy fluctuations during the initial transient phase.[3] After optimizing the rise time we obtained the energy and current waveforms of Fig. 3. Corrections to the non-uniform kinetic energy have been built in to the accelerating schedule and we will see below that by gap 8 these errors have been removed.

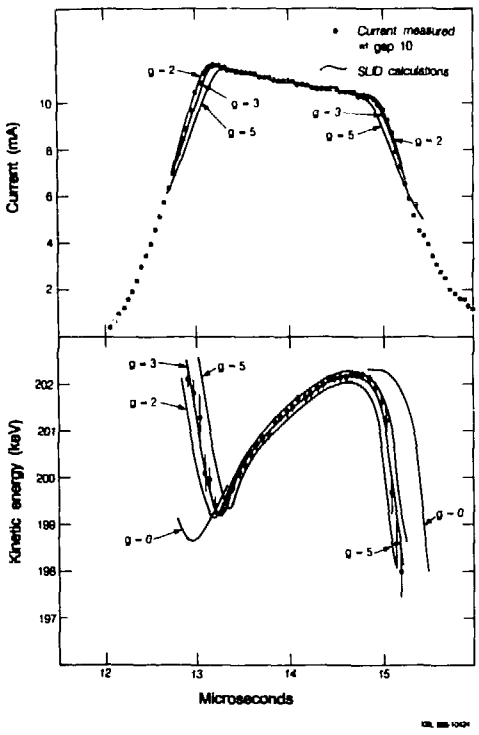

Fig. 4. Empirical determination of the g-factor. Computations of the longitudinal dynamics of a drifting bunch through sections A and B, beginning with the initial conditions of Fig. 3 and using various values of g, are compared to the measured kinetic energy and current waveforms at gap 10.

Because the longitudinal space charge forces are crucial to the operation of the accelerator, it is necessary to determine the degree to which they are reduced by the surrounding conductors. The bunch is 1.4 m long in an electrostatic quadrupole structure with half period nine inches. We employ the long wavelength approximation in which the longitudinal electric field due to space charge is written

$$E = \frac{-g\,\frac{\partial \lambda}{\partial z}}{4\pi\varepsilon_0 \gamma^2}$$

where λ is the line charge density and g is a geometrical factor to be determined. A theoretical estimate of g = 3.4 has been made and an empirical determination is presented here. Figure 4 shows the measured current and kinetic energy waveforms at the end of section B (gap 10) for a drifting beam. Calculations, which begin with the measured initial waveforms at gap 0 (Fig. 3), are also shown using various values of g. Comparison with the data gives g = 2.8 (± 0.6).

MBE-4 can be tuned to various current amplification and acceleration schedules. Here we will confine the discussion to one schedule which begins with an 11 mA current pulse of 2.5 microseconds duration at 200 keV and which accelerates at the limiting rate set by the amount of induction core on each accelerating gap. The accelerating voltage, which is proportional to the rate of change of flux in the core, appears across the gap until the core material saturates, so that the amount of core can be measured in volt-seconds of acceleration. Table I shows the core and pulsing circuits installed at present. Typically between 60% and 80% of these volt-seconds are used to accelerate beam (see Fig. 5).

The design calculations which specify the accelerating waveforms required at each gap to achieve a desired acceleration and amplification schedule have been described elsewhere.[4] Briefly, they take the form of a one dimensional simulation using fifty particles, accelerated at discrete gaps and interacting amongst themselves according to the charge they carry. A computer program called SLID has been developed by C. Kim. At each accelerating gap the computer takes the current and kinetic energy waveforms before acceleration and generates the accelerating waveform

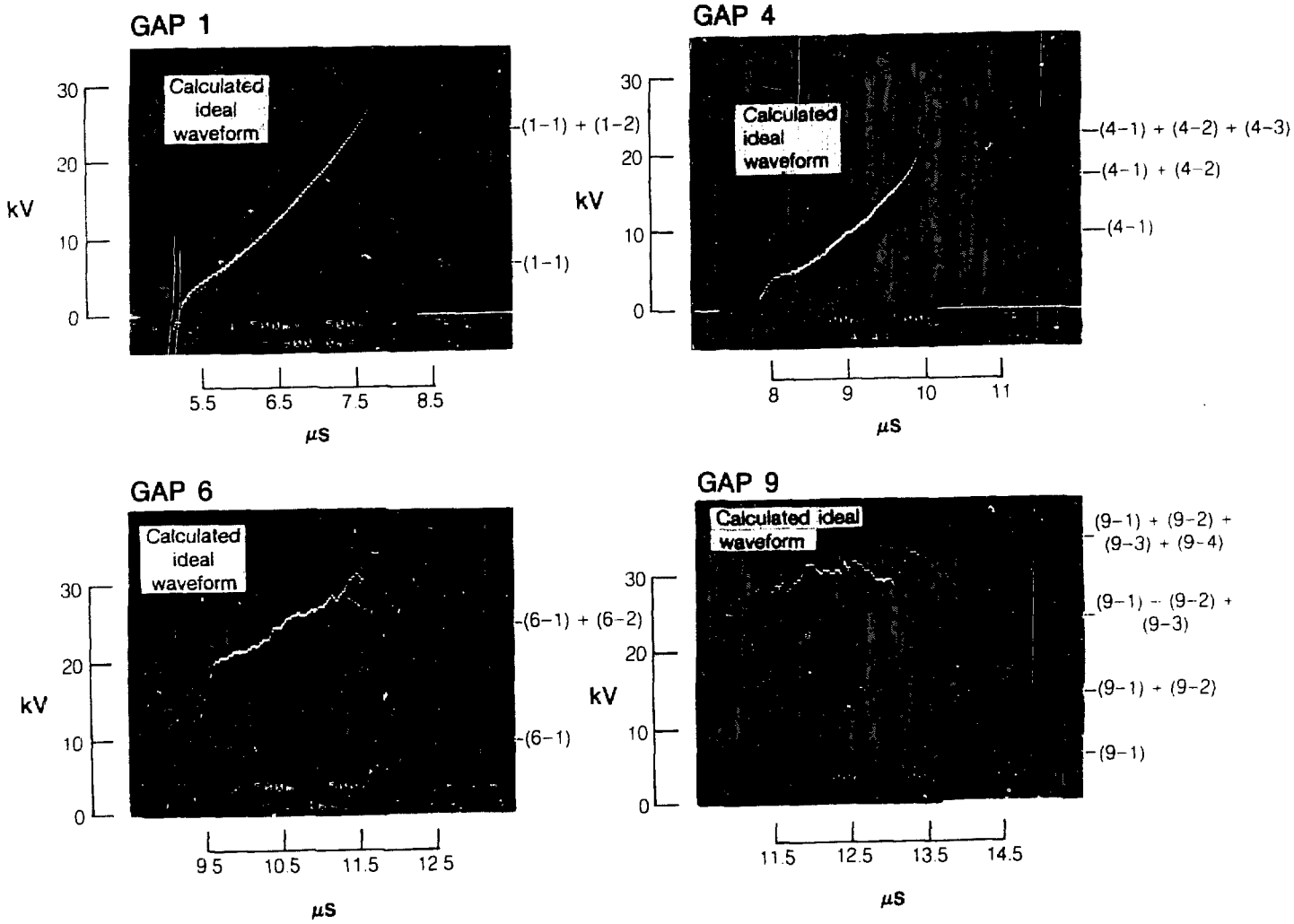

Fig. 5. Actual and ideal waveforms on some of the accelerating gaps. Note the tail corrections at gaps 4 and 9 and the tailored risetime to corect the head at gap 6.

Table 1. Core and Pulsers

gap	pulser	max kV	mV-sec	gap	pulser	max kV	mV-sec
1	1-1	20	40.8	6	6-1	20	47.8
	1-2	10	20.4		6-2	20	40.8
2	2-1	20	40.8	7	7-1	20	47.8
	2-2	10	20.4		7-2	20	40.8
3	3-1	20	40.8	8	8-1	20	47.8
	3-2	10	20.4		8-2	20	40.8
4	4-1	20	40.8	9	9-1	20	47.8
	4-2	10	20.4		9-2	10	23.9
	4-3	10	13.6		9-3	10	23.9
					9-4	10	20.4

needed to change the kinetic energy so as to preserve the shape of the current waveform while amplifying the current. These are known as 'ideal' accelerating waveforms as opposed to the 'actual' waveforms delivered by the pulsers. In the computation the bunch is accelerated according to the ideal waveform at the gap and travels to the next gap. Thus the shape of the inital current waveform (Fig. 3) is preserved through the accelerator while the current and kinetic energy increase. This is known as 'current self-replication'.

At the bunch ends the longitudinal space charge forces are particularly strong and the computation naturally prescribes shaped accelerating waveforms to hold the bunch ends together.

The computed ideal waveforms are approximately triangular in section A, rising from zero as the head of the bunch passes the gap. Thus the head is not accelerated until section B, where the computed ideal accelerating waveforms are approximately flat and the tail of the bunch is in the accelerator.

Careful tuning of the actual accelerating waveforms is required in order to minimise longitudinal emittance growth during acceleration. The procedure we have developed couples the computations with the measurements of the actual waveforms generated at the accelerating gaps. The computation begins with the measured initial conditions (Fig. 3) and generates ideal waveforms for the first three gaps. (The ideal waveform for the first gap includes large corrections to the bunch ends to compensate for the diode transient errors. In practice these errors cannot be corrected at a single gap). The ideal waveforms are written to the screen of a digital oscilloscope where they can be directly compared to the actual waveforms produced across the gaps by the high voltage pulsers. The pulser amplitudes and timing are varied to give actual accelerating waveforms which best match the computed ideal.

Computations of the ideal waveform for a subsequent gap again begin with the initial conditions at gap 0 shown in Fig. 3. The equations of motion are integrated from gap 0 to the gap of interest using digitised measurements of the actual accelerating waveforms applied across the intervening gaps, then the ideal waveform for the gap of interest is

computed. For example, the computation of the ideal waveform on gap 9 involves integration of the equations of motion from gap 0 to gap 9 using the actual accelerating waveforms applied across gaps 1 - 4, 6 - 8. At the last of the four gaps of each accelerator section (gaps 4 and 9 for that part of MBE-4 already constructed) we install additional pulsers to control the space charge at the bunch ends and compensate as best we can for errors in the previous gaps (Table I). Figure 5 shows the results for gaps 1, 4, 6 and 9.

The shaping of the accelerating waveforms to control the bunch ends is dominated at first by the corrections for the transient effects in the diode. The transient error at the tail of the bunch is corrected at gap 4 (see Fig. 5 where the actual waveform on gap 4 matches the ideal all the way to the tail of the bunch).

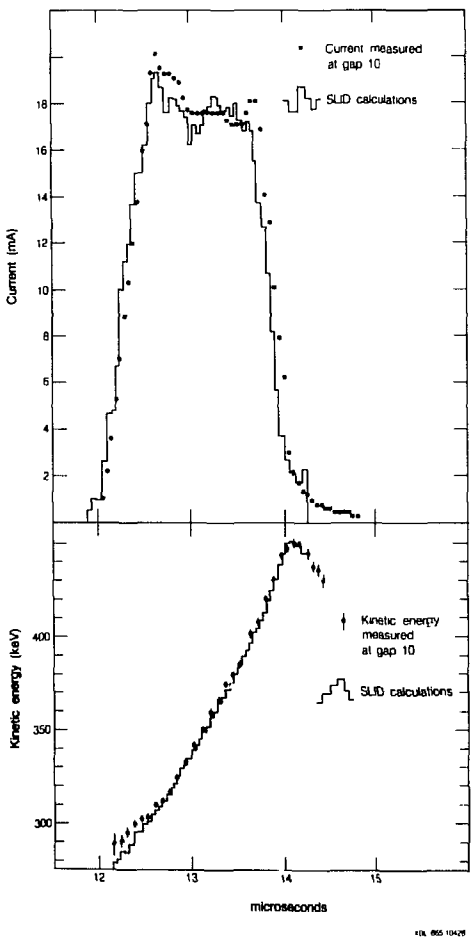

Fig. 6. Measured and calculated current and kinetic energy waveforms for the right beam at the end of section B, under the accelerating schedule described here. Current is amplified by a factor of 1.6. All the errors caused by the diode transients are corrected.

The transient error at the head of the bunch calls for deceleration relative to the rest of the ions. Deceleration of the head of the bunch by means of negative voltage pulses with tailored trailing edges has not proved possible. The trailing edge occurs when the core material is beginning to saturate, the impedance is changing and the circuit design is very difficult. Instead, the bunch head is corrected by refraining from accelerating it on gaps 6, 7 and 8, by means of a tailored rising edge on the main accelerating waveform. Figure 5 shows such a waveform on gap 6, here the ideal is computed using the actual waveforms on gaps 1 - 4. The required fast rise-times at gaps 6, 7 and 8 cause some oscillation of the actual accelerating waveforms so that the match to the ideal in section B is not as good as that achieved in section A.

Since the ideal waveform for gap 9 is calculated using the actual waveforms applied to gaps 1 - 4, 6 - 8, this computation calls for corrections for all the errors on the previous gaps and represents a measure of the cumulative error. The frequency of the cumulative error is too high for corrections to actually be

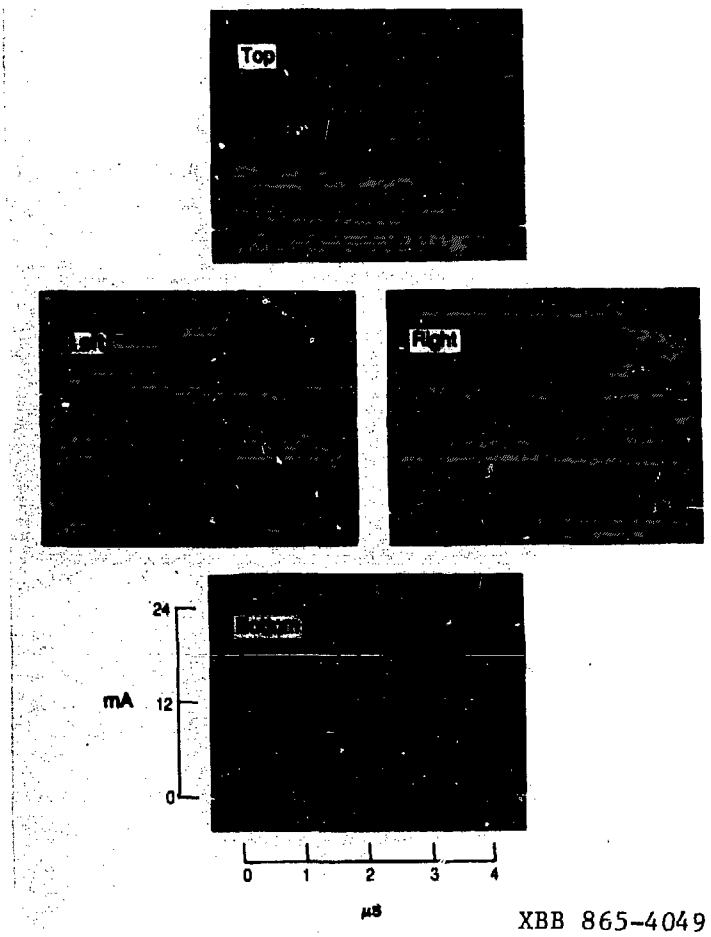

Fig. 7. Initial and final current waveforms for all four beams. Current self-replication is not working perfectly. The modulations of the final current waveform are caused primarily by very small voltage errors on gaps 1-4, which have excited space charge waves.

made and the amplitude, after 7 gaps, is about 2 kV. However the beam is not sensitive to frequency components of the errors above about 2 MHz, integrated over the transit time through the gap (300 ns). The cumulative error of 2 kV thus represents an upper limit on the degradation of longitudinal emittance.

Figure 6 shows the current and kinetic energy waveforms at gap 10, after acceleration. Slow changes of kinetic energy through the bunch are part of the acceleration schedule; there are no high-frequency uncorrectable errors visible within the resolution of the measurement. This sets a limit of about 2 keV on the amplitude of uncorrectable errors after 8 gaps.

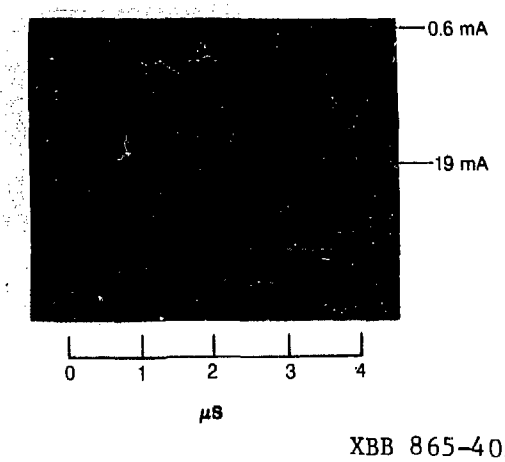

Fig. 8. Comparison of current modulations caused by small acceleration errors at the early gaps on a) space charge dominated 10 mA beam and b) 0.6 mA beam with negligable self-forces.

In the context of a heavy ion fusion driver the acceptable longitudinal emittance is determined by the final lens system and the focal spot requirements. If one imagines random errors on each gap which, through a long accelerator, accumulate as the square root of the number of gaps, one could tolerate uncorrectable voltage errors at about one percent of the accelerating voltage.[5] Our measurements to date indicate that MBE-4 operates just within this limit. The situation will be clearer when the experiment is longer.

Pulser voltage errors soon become beam current fluctuations. In Fig. 7 the initial and final current waveforms are compared for all four beams. Current is amplified by a factor of 1.6. The final current waveforms show modulation which is caused by the voltage errors in the first few gaps. In Fig. 8 we compare the modulations on the standard 11-18 mA beam with those on a low space charge beam starting at 0.6 mA. The modulations are clearly less for the space charge dominated beam.

LONGITUDINAL/TRANSVERSE COUPLING

The r.m.s. transverse emittance is derived from measurements of the transverse phase space distributions. A pair of slits, one defining x, the other defining x', are moved across the beam from pulse to pulse and the transmitted current is measured. We find $\varepsilon = 1.5 \pm 0.3 \times 10^{-7}$ π m rad where ε is defined by the expression.

$$\pi\varepsilon \equiv 4\pi\beta\gamma \left[\langle x^2 \rangle \langle x'^2 \rangle - \langle xx' \rangle^2 \right]^{1/2}$$

The K-V envelope equations[6] describe the beam size during acceleration quite well. We integrate the envelope equations beginning with measured initial r.m.s. radii and divergences at gap 0. At each accelerating gap the kinetic energy, current and beam envelopes are changed discretely according to the accelerating schedule of the head or tail of the bunch. For the head we take a point in the bunch which arrives at gap 10 12.8 μs after the Marx fires (see Fig. 6); for the tail we take 13.7 μs. The quadrupole strength is set to preserve the centre of the bunch at $\sigma_0 = 60°$ as the kinetic energy increases. This calculation proceeds through the ten quadrupole periods of section A and B and is compared in Fig. 9 to the phase space distributions measured at gap 10. The agreement is good and the K-V calculations reproduce the different optics of the head and tail.

The beam size is not strongly dependent on kinetic energy if the current is constant; as the kinetic energy increases from head to tail of the bunch at constant current the increased stiffness is approximately compensated by the decreased perveance. In the acceleration schedule implemented here the current has the same magnitude throughout the bunch as it passes a given point in the accelerator (Figs. 3 and 6), thus the equilibrium size of the head is close to the equilibrium size of the tail, both staying close to their initial values during acceleration. The upper part of Fig. 9 shows the calculated beam envelopes during acceleration through the ten quadrupole doublets of sections A and B. Mismatch oscillations, which can be seen as changes in the maximum beam size, are not a significant problem.

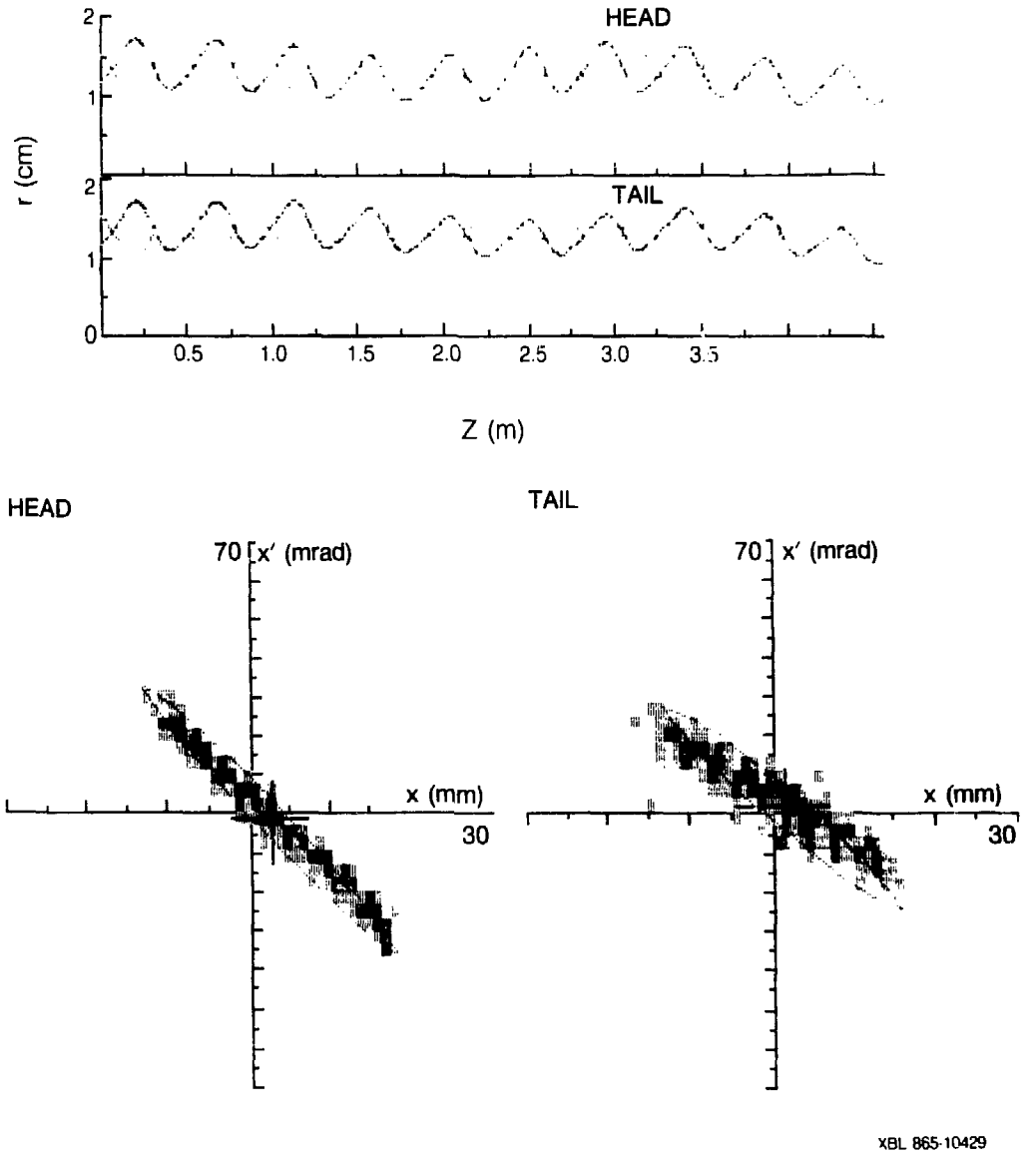

Fig. 9. Behaviour of the envelopes during acceleration. Integration of the K-V envelope equations through the ten periods of section A and B,beginning with measured initial conditions, are shown for the head and tail of the bunch. In the lower part of the Fig. the final K-V ellipses are compared to phase space distributions measured at gap 10.

SUMMARY

MBE-4 is an experiment which has just begun. The achievement to date has been to implement an acceleration schedule and observe that the transverse and longitudinal dynamics behave as calculated. The beams have been shown not to interact with one another, the current has been amplified by a factor of 1.6 with tolerable longitudinal energy errors,

bunch end control has been implemented and mismatch oscillations have been investigated and found to be small.

Important questions have still to be answered regarding the effects of misalignments, preservation of transverse emittance and the possibility of making steering corrections during acceleration. We need to refine our techiques to follow the transverse emittance as the angles become smaller during acceleration. We also need to improve the resolution of tne energy measurements to detect longitudinal energy errors in the beam itself. The development of longitudinal errors will be particularly interesting as the accelerator gets longer. Current fluctuations are of great interest, but MBE-4 will not operate in the regime of high beam currents where fluctuations may grow due to coupling through the impedance of the structure.

REFERENCES

1. R.T Avery et al., IEEE Trans. Nucl. Sci., NS-32 (1985) 3187.
   A.I. Warwick, D. Vanecek and O. Fredriksson, IEEE Trans. Nucl. Sci., NS-32 (1985) 3196.

2. HIFAR Year End Report, LBL-20310 (1985).

3. M.G. Tiefenback and M. Lampel, Appl. Phys. Lett., 143-1 (1983), 57.

4. C. Kim and L. Smith, Particle Accelerators, 18 (1985) 101.

5. D. L. Judd, Proc. Heavy Ion Fusion Workshop, LBL-10301, (1979).
   E.P. Lee, private communication.

6. F. Sacherer, IEEE Trans. Nucl. Sci., NS-18 (1971) 1105.